crystals

MDPI

Communication

Single Crystal Growth and X-ray Diffraction Characterization of a Quasi-Spin Chain Compound, Li_2CuO_2

Ashiwini Balodhi and Min Gyu Kim *

Department of Physics, University of Wisconsin-Milwaukee, Milwaukee, WI 53201, USA; balodhia@uwm.edu
* Correspondence: mgkim@uwm.edu

Abstract: We report the growth of single crystals and X-ray diffraction characterization of the quasi-one-dimensional spin chain compound, Li_2CuO_2. The single crystals were grown using the high-temperature solution growth technique. The resulting blade-shaped crystals exhibit a shiny black color, with dimensions reaching several millimeters along the crystallographic *b*-axis. The as-grown crystals were characterized using powder X-ray diffraction and Laue back reflection. The I-centered orthorhombic, *Immm*, structure was confirmed. Crystal structure parameters were determined to be a = 3.6744 Å, b = 2.8600 Å, and c = 9.4257 Å from Rietveld analysis. Our work helps to remove obstacles to the synthesis and study of a model cuprate system, Li_2CuO_2, facilitating the use of experimental probes that require sizable crystals.

Keywords: quasi one dimensional materials; frustrated spin chain; low dimensional magnet

check for updates

Citation: Balodhi, A.; Kim, M.G. Single Crystal Growth and X-ray Diffraction Characterization of a Quasi-Spin Chain Compound, Li_2CuO_2. *Crystals* **2024**, *14*, 288. https://doi.org/10.3390/cryst14030288

Received: 4 March 2024
Revised: 11 March 2024
Accepted: 15 March 2024
Published: 21 March 2024

1. Introduction

Intense research focus in low-dimensional materials centers around one-dimensional (1D) spin chains (e.g., Sr_2CuO_3, $CuGeO_3$, $SrCuO_2$) and spin ladders (e.g., $Sr_{14}Cu_{24}O_{41}$, $SrCu_2O_3$) [1–3], owing to a myriad of unusual low-temperature properties governed by quantum effects. Refs. [2–4] These properties include various types of magnetic ground states for half-integer [5–7] and integer spin systems (e.g., the Haldane chain) [8,9], as well as the separation of spin (spinon) and charge (holon) degrees of freedom in Sr_2CuO_3 [10–13], spin-Peierls transitions in $CeCuGe_3$ [14], etc. These phenomena are entirely governed by quantum-mechanical behavior and lack three-dimensional analogs. As observed, compounds containing, $S = 1/2$, Cu^{2+}, ions offer an excellent experimental platform for realizing such networks [1–3,5–7,10–14] because of the enhanced quantum fluctuations resulting from Cu^{2+} ions and reduced dimensionality.

Recently, there has been considerable interest in the quasi 1D compound, Li_2CuO_2. Refs. [15–22] Li_2CuO_2 crystallizes into an orthorhombic structure (*Immm*, space group #71) with a = 3.6544 Å, b = 2.8602 Å, and c = 9.3774 Å at ambient pressure. Refs. [23,24] As depicted in Figure 1a, the most notable characteristic of Li_2CuO_2 is the formation of quasi-one-dimensional linear chains composed of CuO_2 along the *b*-axis, separated by Li-O groups along the *c*-axis. Refs. [24,25] Due to the simple CuO_4 square planar coordination along the *b*-axis (see Figure 1b), these spin chains run parallel to each other with a Cu-O-Cu bond angle of approximately 94°. Refs. [24,26] The copper atoms within these structural chains exhibit ferromagnetic (FM) coupling, resulting in ferromagnetic alignment along the *b*-axis, which are antiferromagnetically (AFM) coupled between the neighboring chains in the *c*-axis. Refs. [17,24,26] The remarkable interplay between one and three-dimensional magnetic interactions distinguishes Li_2CuO_2 from other related compounds, as evidenced by, for instance, the presence of long-range AFM order observed below $T_N \approx 9$ K with a Curie-Weiss temperature, $\Theta_{cw} = -42$ K, ref. [24] a field-induced weak ferromagnetic component below $T_2 > 2.6$ K, refs. [27,28] and relatively large magnetic moments of O^{2-} ions in Li_2CuO_2 of about 0.2 μ_B (largest for any low-dimensional cuprate system), and Zhang-Rice

type excitations. Refs. [29,30] Despite the tremendous theoretical [15,19,20,27] and experimental studies, refs. [15,17,24,26,27] the precise nature of the magnetic interactions in this charge transfer insulator [31–33] has remained a topic of contentious debate.

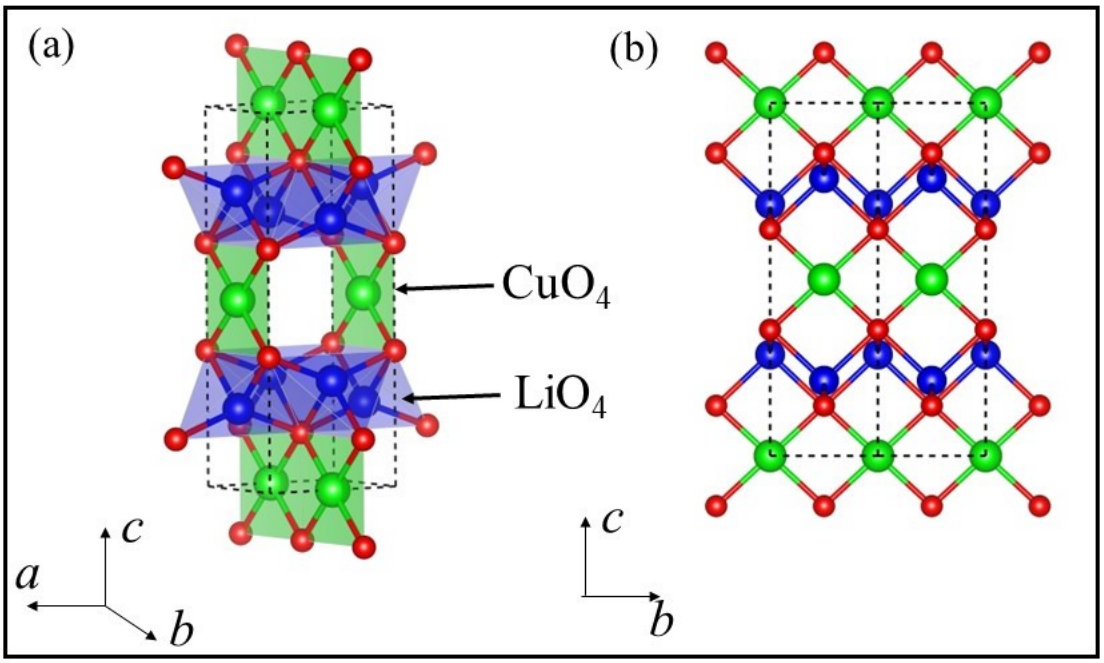

Figure 1. (**a**) Schematics of a unit cell of Li_2CuO_2. The magnetic moments within the CuO_2 planes along *b*-axis are FM ordered, whereas neighboring planes are coupled AFM along the *c*-axis. Red full circles are the oxygen atoms, green color circles are the Cu atoms and the blue circles are the Li atoms. Solid bicolor lines are the nearest neighbor Cu-O and Li-O bonds. (**b**) Schematics of a two unit cell of Li_2CuO_2 in the *bc* plane.

It is noteworthy that most studies have focused on polycrystalline, Li_2CuO_2. Refs. [23,24,27,34,35] Bulk characterizations were done on single crystals grown by the floating-zone (FZ) technique. Refs. [16,18,26,28,30,33,36] These single crystals were grown under partial oxygen pressure and exhibited some oxygen vacancies. This oxygen partial pressure can strongly influence the Lithium self-diffusion, leading to the formation of $Li_2CuO_{2-\delta}$, where $\delta = 0 - 0.3$, within their structure. Refs. [16,18] Consequently, the magnetic susceptibility, $\chi(T)$, data at low temperatures for these single crystals of Li_2CuO_2 exhibit a slightly more pronounced Curie-like increase, which varies between samples, suggesting possible sample contamination related to surface sensitivity to moisture. Refs. [16–18] This variation may stem from differences in the thickness of inclusions of the second phase or micro-cracks at cleaved planes. Ref. [18] Given that advanced FZ techniques are not widely available in most scientific laboratories, we were inspired to investigate the synthesis of Li_2CuO_2 using the more accessible high-temperature solution growth technique, also known as the flux method.

Here, we present a successful single crystal growth of Li_2CuO_2. We utilized a conventional flux method and synthesized blade-shaped single crystals which are shiny black in color and air-sensitive [18], with dimensions reaching up to several millimeters along the crystallographic *b*-axis. We demonstrate the high quality of our single crystals through X-ray diffraction characterization. To the best of our knowledge, we present the first instance of Li_2CuO_2 crystal growth via flux growth.

2. Materials and Methods

Single crystals of Li_2CuO_2 were grown using Li_2CO_3 flux. The precisely weighed starting materials, Li_2CO_3 (99.999%, Alfa Aesar, Haverhill, MA, USA), and CuO (99.995%,

Alfa Aesar), were homogeneously mixed in a 4:1 ratio. This mixture was carefully transferred into an alumina crucible, covered with a lid, and gradually heated to 900 °C over 5 h, and held at 900 °C for 72 h (3 days) in air. Finally, the furnace was slowly cooled to room temperature for over 30 h. We obtained blade-shaped shiny single crystals (shown in Figure 2) with typical dimensions of 3 × 0.3 × 0.1 mm^3.

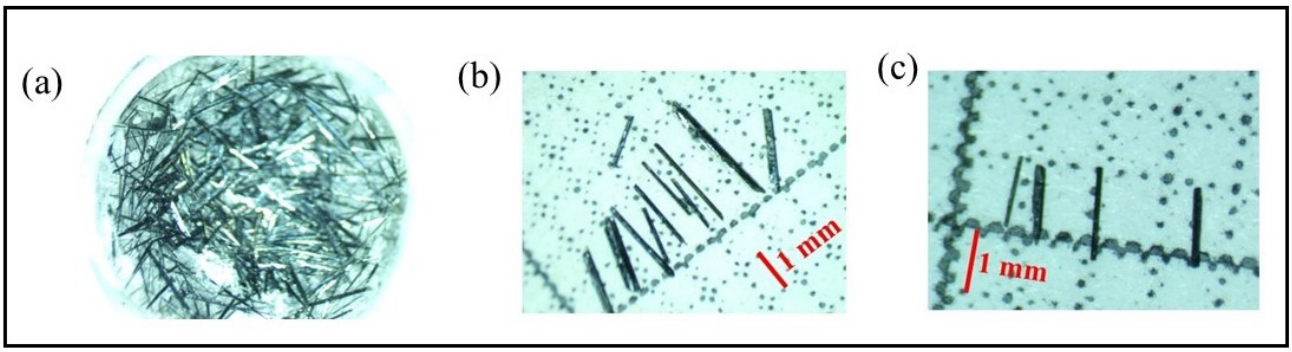

Figure 2. (**a**) As-grown single crystals of Li_2CuO_2 in the flux matrix. (**b**,**c**) Single crystals pulverized from the flux matrix of Li_2CuO_2 from two different batches on a millimeter-sized grid.

We studied the crystal structure and the purity of the single crystal Li_2CuO_2 using powder X-ray diffraction (PXRD). The PXRD patterns were measured on pulverized Li_2CuO_2 single crystals at room temperature using a Proto AXRD Benchtop powder diffractometer. We utilized Cu-K_α X-ray radiation, and the structure was quantitatively analyzed by the Rietveld method using the GSAS program package [37].

We identified the crystallinity and crystallographic orientations of our single crystals using a Proto Laue-COS system, utilizing the Laue back reflection method. We used the Cu X-ray tube for X-ray generation with 40 kV and 30 mA. Due to the small width of the blade, we used a 0.8 mm pinhole aperture. We mount the single crystal with one of the flat surfaces perpendicular to the incident X-rays and the long blade direction vertically. Approximately 16 scans were performed over an extended duration (8 min) and averaged for clear diffraction patterns. The Laue patterns were analyzed by the Cologne Laue Indexation Program (CLIP) [38].

3. Results and Discussions

3.1. Single Crystal Growth

Figure 2a displays optical images of as-grown single crystals in the flux matrix as well as two separate batches of pulverized Li_2CuO_2 single crystals on a millimeter-sized grid (see Figure 2b,c). This demonstrates that our synthesis conditions are highly reproducible. In the flux matrix, we obtained black, shiny blade-shaped single crystals with dimensions typically ranging from 2–3 mm in length, 0.3 mm in width, and 0.1 mm in thickness, with the longest dimension aligned along the crystallographic *b*-axis (see Laue X-ray diffraction below).

3.2. Structural Characterizations

To determine the crystal structure of the as-grown Li_2CuO_2 single crystals, we conducted single crystal diffraction and PXRD measurements in the Bragg-Brentano geometry at room temperature. Figure 3a displays the single crystal diffraction pattern. We observed peaks corresponding to the (1, 0, 1) and (2, 0, 2) planes at approximately 2θ values of 25.96° and 53.48°, respectively. Earlier studies done on the single crystalline samples (using FZ technique) by Chung et al. [22] showed the resulting crystalline boules were faceted and exhibited a tendency to cleave along (1, 0, 1) planes similar to our single crystals [33]. It is consistent with an orthorhombic structure within the *Immm* group in Ref. [24] and our analysis below.

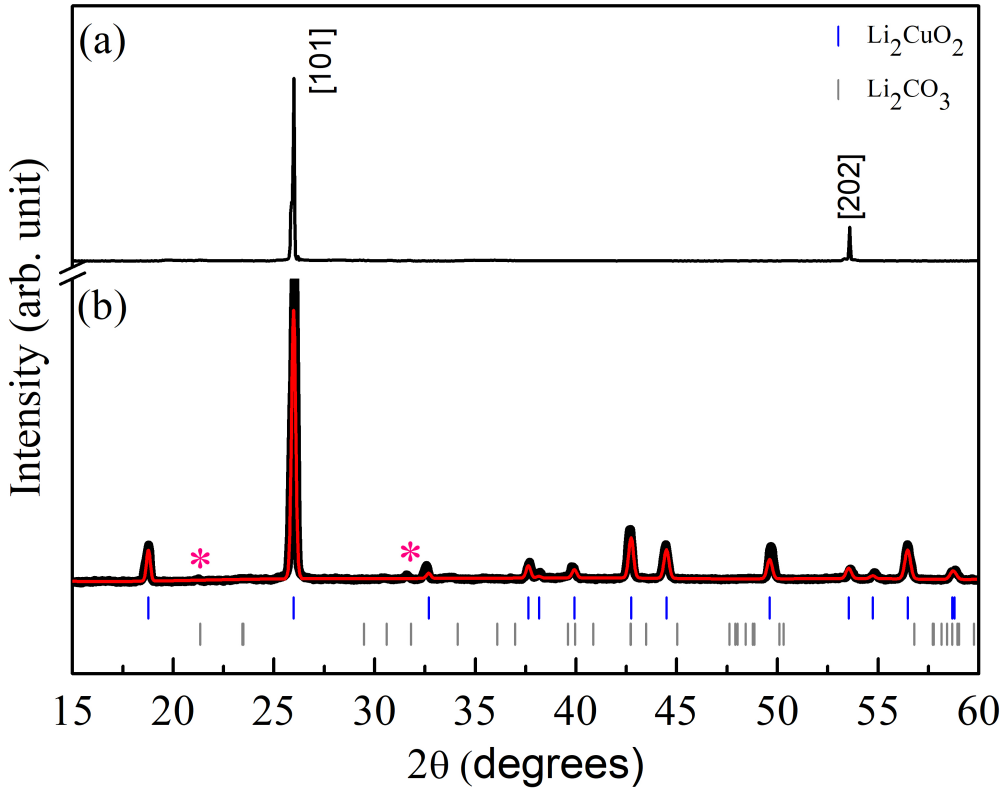

Figure 3. (Color online) (**a**) Single crystal X-ray diffraction pattern of Li_2CuO_2. (**b**) Powder X-ray diffraction pattern (black) of pulverized single-crystals of Li_2CuO_2. The solid (red) curves overlaying the data represent the fit from Rietveld refinement. The blue and grey solid lines represent the reference peaks of Li_2CuO_2 and Li_2CO_3, respectively. The * symbols show the impurity peaks of a flux component, Li_2CO_3.

The PXRD pattern of the pulverized Li_2CuO_2 single crystals from the crystal batch in Figure 2c are displayed in Figure 3b. We performed detailed structural refinement using the structure model described in ref. [24]. The solid (red) curves overlaid on the data represent the Rietveld refinement in Figure 3b. We found that the PXRD pattern predominantly consists of the correct Li_2CuO_2 phase. We determined the lattice parameters of Li_2CuO_2 to be a = 3.67442 Å, b = 2.86001 Å, c = 9.42566 Å with $\alpha = \beta = \gamma = 90°$, and we obtained the goodness-of-fit parameters χ^2 = 3.785 and R_{wp} = 0.584. Our Rietveld result is consistent with the orthorhombic *Immm*. The atomic coordinates and other parameters considered for the measurements, as well as detailed refined parameters for Li_2CuO_2, are presented in Table 1. These values agree well with previously reported values [24,34] as shown in Table 2. We found a small amount of impurity (less than 4%) in the PXRD pattern. It is determined to be the flux component Li_2CO_3 (ICSD: 66941), appearing at 2θ = 21.1976° and 31.5°, indicated by * (dark grey) in Figure 3b.

Table 1. Structural parameters obtained by refining X-ray powder diffraction for Li_2CuO_2 at room temperature, shown in Figure 3b with a space group *Immm* (#71). The I-centered orthorhombic lattice constants are a = 3.6744 Å, b = 2.8600 Å, c = 9.4257 Å, and $\alpha = \beta = \gamma = 90°$, with goodness of fit parameters, χ^2 = 3.785, and R_{wp} = 0.584.

Atom	Wyck	*x*	*y*	*z*	*Occ.*	*B* (Å)
Li	4j	0.5	0	0.18487	1	0.00032
Cu	2b	0	0.5	0.5	1	0.00032
O	4i	0	0	0.36189	1	0.00032

Table 2. Comparison of the experimental and computed lattice constants, *a*, *b*, and *c* for Li_2CuO_2 in the current study and literature data.

	a (Å)	*b* (Å)	*c* (Å)	Cu-O-Cu (°)	Cu-Cu (Å)	Cu-O (Å)	Reference
Experiment	3.6744	2.8600	9.4257	95.37	2.8600	1.9338	this work
Experiment	3.6615	2.8627	9.3925	93.96	2.8628	1.9577	Ref. [24]
Experiment	3.65	2.86	9.38	-	-	-	Ref. [34]
Experiment	3.6614	2.8648	9.3969	91		1.987	Ref. [16]
Experiment: $Li_2CuO_{1.71}$	3.6609	2.8638	9.3934	95.55	-	-	Ref. [16]
DFT, GGA + PBE	3.5779	2.8628	9.3926	-	-	1.9162	Ref. [21]

3.3. Laue X-ray Diffraction

We examined the crystallinity of our crystal selected from the batch shown in Figure 2b, using the Laue back reflection method across the as-grown crystal facet. The resulting Laue image from a Li_2CuO_2 single crystal is shown in Figure 4a and simulated Laue patterns together with the data are presented in Figure 4b. Our Laue pattern shows no visible impurity phases or misaligned crystals, indicating a high quality of the single crystal. We find that the surface perpendicular to the incident X-rays is (1, 0, 1) plane, and the horizontal direction is the high symmetry direction to (1, 0, 0). We also find that the vertical direction is to [0, 1, 0], which is along the long blade direction. Considering the proposed quasi-one-dimensional chains in this compound, it is natural that the crystal extends along the chain direction (the crystallographic *b*-axis).

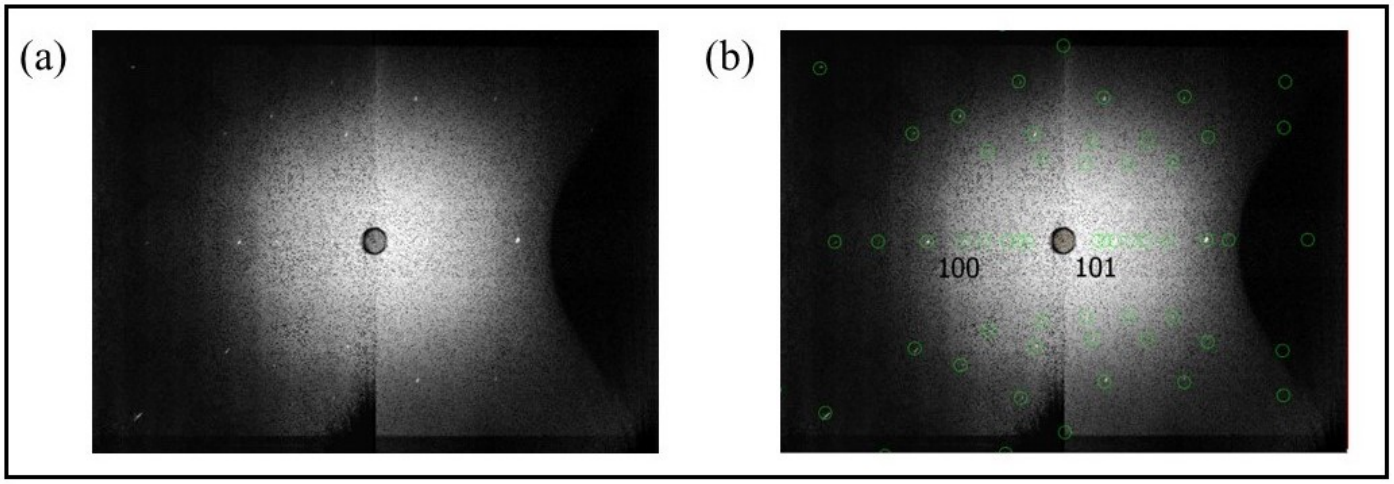

Figure 4. (**a**) Laue diffraction pattern for Li_2CuO_2 single crystal along the (100) direction. (**b**) Laue diffraction pattern with simulated diffraction pattern in green circles by using Cologne Laue Indexation Program (CLIP) software (version CLIP4 RC1). (100) and (101) directions are marked. The vertical direction is (010) direction.

4. Conclusions

We present a comprehensive report on the single crystal growth using the flux method and the structural characterization of Li_2CuO_2 single crystals. Through a detailed structural refinement of the PXRD diffraction data, we determine that the material crystallizes in a *Immm* (#71) space group, with orthorhombic symmetry, and assess the lattice parameters of Li_2CuO_2. Our observations indicate that the as-grown samples of Li_2CuO_2 measure several millimeters along the crystallographic *b*-axis. Further, Laue back reflection X-ray measurements indicate the high quality of the single crystal. Our work helps to remove obstacles to the synthesis and study of a model cuprate system, Li_2CuO_2, facilitating the use of experimental probes that require sizable crystals.

Author Contributions: Conceptualization, A.B.; methodology, A.B. and M.G.K.; validation, A.B. and M.G.K.; formal analysis, A.B.; investigation, A.B. and M.G.K.; resources, M.G.K.; data curation, A.B. and M.G.K.; writing—original draft preparation, A.B. and M.G.K.; writing—review and editing, A.B. and M.G.K.; visualization, A.B.; supervision, M.G.K.; project administration, M.G.K.; funding acquisition, M.G.K. All authors have read and agreed to the published version of the manuscript.

Funding: This work is supported by the University of Wisconsin-Milwaukee.

Data Availability Statement: The data supporting this study's findings are available within the article.

Conflicts of Interest: The authors declare no conflicts of interest.

References

1. Schulz, H. *Correlated Fermions and Transport in Mesoscopic Systems*; Martin, T., Montambaux, G., Tran Thanh Van, J., Eds.; Editions Fronti'eres: Gif-sur-Yvette, France, 1996.
2. Giamarchi, T. *Quantum Physics in One Dimension*; Clarendon Press: Oxford, UK, 2004.
3. Rice, T.M. The rich variety of cuprates. *Phys. B Condens. Matter* **1997**, *241–243*, 5–12. [CrossRef]
4. Vasiliev, A.; Volkova, O.; Zvereva, E.; Markina, M. Milestones of low-D quantum magnetism. *npj Quantum Mater.* **2018**, *3*, 18. [CrossRef]
5. Dagotto, E. Experiments on ladders reveal a complex interplay between a spin-gapped normal state and superconductivity. *Rep. Prog. Phys.* **1999**, *62*, 1525. [CrossRef]
6. Johnston, D.C.; Kremer, R.K.; Troyer, M.; Wang, X.; Klümper, A.; Bud'ko, S.L.; Panchula, A.F.; Canfield, P.C. Thermodynamics of spin S = 1/2 antiferromagnetic uniform and alternating-exchange Heisenberg chains. *Phys. Rev. B* **2000**, *61*, 9558. [CrossRef]
7. Cowley, R.A. *Dynamical Properties of Unconventional Magnetic Systems*; NATO ASI Series; Springer: Dordrecht, The Netherlands, 1998; Volume 349.
8. Haldane, F.D.M. Nonlinear Field Theory of Large-Spin Heisenberg Antiferromagnets: Semiclassically Quantized Solitons of the One-Dimensional Easy-Axis Néel State. *Phys. Rev. Lett.* **1983**, *50*, 1153. [CrossRef]
9. Honda, Z.; Asakawa, H.; Katsumata, K. Magnetic Field versus Temperature Phase Diagram of a Quasi-One-Dimensional S = 1 Heisenberg Antiferromagnet. *Phys. Rev. Lett.* **1998**, *81*, 2566. [CrossRef]
10. Schlappa, J.; Wohlfeld, K.; Zhou, K.J.; Mourigal, M.; Haverkort, M.W.; Strocov, V.N.; Hozoi, L.; Monney, C.; Nishimoto, S.; Singh, S.; et al. Spin–orbital separation in the quasi-one-dimensional Mott insulator Sr_2CuO_3. *Nature* **2012**, *485*, 82–85. [CrossRef] [PubMed]
11. Johnston, S.; Monney, C.; Bisogni, V.; Zhou, K.-J.; Kraus, R.; Behr, G.; Strocov, V.N.; Malek, J.; Drechsler, S.-L.; Geck, J.; et al. Electron-lattice interactions strongly renormalize the charge-transfer energy in the spin-chain cuprate Li_2CuO_2. *Nat. Commun.* **2016**, *7*, 10563. [CrossRef]
12. Fujisawa, H.; Yokoya, T.; Takahashi, T.; Miyasaka, S.; Kibune, M.; Takagi, H. Angle-resolved photoemission study of Sr_2CuO_3. *Phys. Rev. B* **1990**, *59*, 7358. [CrossRef]
13. Kim, C.; Matsuura, A.Y.; Shen, Z.-X.; Motoyama, N.; Eisaki, H.; Uchida, S.; Tohyama, T.; Maekawa, S. Observation of Spin-Charge Separation in One-Dimensional $SrCuO_2$. *Phys. Rev. Lett.* **1996**, *77*, 4054. [CrossRef]
14. Hase, M.; Terasaki, I.; Uchinokura, K. Observation of the spin-Peierls transition in linear Cu^{2+} (spin-1/2) chains in an inorganic compound $CuGeO_3$. *Phys. Rev. Lett.* **1993**, *70*, 3651. [CrossRef] [PubMed]
15. Zoghlin, E.; Stone, M.B.; Wilson, S.D. Refined spin-wave model and multimagnon bound states in Li_2CuO_2. *Phys. Rev. B* **2023**, *108*, 064408. [CrossRef]
16. Shu, G.J.; Tian, J.C.; Lin, C.K.; Hayashi, M.; Liou, S.C.; Chen, W.T.; Wong, D.P.; Liou, H.L.; Chou, F.C. Corrigendum: Oxygen vacancy-induced magnetic moment in edge-sharing CuO_2 chains of $Li_2CuO_{2-\delta}$. *New J. Phys.* **2018**, *20*, 059501. [CrossRef]
17. Kuzian, R.O.; Klingeler, R.; Lorenz, W.E.A.; Wizent, N.; Nishimoto, S.; Nitzsche, U.; Rosner, H.; Milosavljevic, D.; Hozoi, L.; Yadav, R.; et al. Comment on 'Oxygen vacancy-induced magnetic moment in edge-sharing CuO_2 chains of Li_2CuO_2. *New J. Phys.* **2018**, *20*, 058001. [CrossRef]
18. Wizent, N.; Behr, G.; Loser, W.; Buchner, B.; Klingeler, R. Challenges in the crystal growth of Li_2CuO_2 and $LiMnPO_4$. *J. Cryst. Growth* **2011**, *318*, 995–999. [CrossRef]
19. Nishimoto, S.; Drechsler, S.-L.; Kuzian, R.; Richter, J.; van den Brink, J. Interplay of interchain interactions and exchange anisotropy: Stability and fragility of multipolar states in spin-1/2 quasi-one-dimensional frustrated helimagnets. *Phys. Rev. B* **2015**, *92*, 214415. [CrossRef]
20. Nishimoto, S.; Drechsler, S.-L.; Kuzian, R.O.; van den Brink, J.; Richter, J.; Lorenz, W.E.A.; Skourski, Y.; Klingeler, R.; Büchner, B. Saturation Field of Frustrated Chain Cuprates: Broad Regions of Predominant Interchain Coupling. *Phys. Rev. Lett.* **2011**, *107*, 097201. [CrossRef]
21. Kordatos, A.; Kuganathan, N.; Kelaidis, N.; Iyngaran, P.; Chroneos, A. Defects and lithium migration in Li_2CuO_2. *Sci. Rep.* **2018**, *8*, 6754. [CrossRef]
22. Chung, E.M.L.; McIntyre, G.J.; Paul, D.M.; Balakrishnan, G.; Lees, M.R. Oxygen moment formation and canting in Li_2CuO_2. *Phys. Rev. B* **2003**, *68*, 144410. [CrossRef]

23. Hoppe, R.; Rieck, H. Die Kristallstruktur von Li_2CuO_2. *Z. Fur Anorg. Und Allg. Chem. Band* **1970**, *379*, 157–164. [CrossRef]
24. Sapiña, F.; Rodríguez-Carvajal, J.; Sanchis, M.J.; Ibáñez, R.; Beltrán, A.; Beltrán, D. Crystal and magnetic structure of Li_2CuO_2. *Solid State Commun.* **1990**, *74*, 779–784. [CrossRef]
25. Sreedhar, K.; Ganguly, P. Magnetic susceptibility studies on ternary oxides of copper(II). *Inorg. Chem.* **1988**, *27*, 2261. [CrossRef]
26. Boehm, M.; Coad, S.; Roessli, B.; Zheludev, A.; Zolliker, M.; Böni, P.; Paul, D.M.; Eisaki, H.; Motoyama, N.; Uchida, S. Competing exchange interactions in Li_2CuO_2. *Europhys. Lett.* **1998**, *43*, 77–82. [CrossRef]
27. Ortega, R.J.; Jensen, P.J.; Rao, K.V.; Sapiña, F.; Beltrañ, D.; Iqbal, Z.; Cooley, J.C.; Smith, J.L. A field induced ferromagnetic-like transition below 2.8 K in Li_2CuO_2 An experimental and theoretical study. *J. Appl. Phys.* **1998**, *83*, 6542–6544. [CrossRef]
28. Staub, U.; Roessli, B.; Amato, A. Magnetic ordering in Li2CuO2 studied by μSR technique. *Phys. B* **2000**, *299*, 289–290. [CrossRef]
29. Learmonth, T.; McGuinness, C.; Glans, P.-A.; Downes, J.E.; Schmitt, T.; Duda, L.-C.; Guo, J.-H.; Chou, F.C.; Smith, K.E. Observation of multiple Zhang-Rice excitations in a correlated solid: Resonant inelastic X-ray scattering study of Li_2CuO_2. *Europhys. Lett.* **2007**, *79*, 47012. [CrossRef]
30. Monney, C.; Bisogni, V.; Zhou, K.-J.; Kraus, R.; Strocov, V.N.; Behr, G.; Málek, J.; Kuzian, R.; Drechsler, S.-L.; Johnston, S.; et al. Determining the Short-Range Spin Correlations in the Spin-Chain Li_2CuO_2 and $CuGeO_3$ Compounds Using Resonant Inelastic X-Ray Scattering. *Phys. Rev. Lett.* **2013**, *110*, 087403. [CrossRef]
31. Mizuno, Y.; Tohyama, T.; Maekawa, S.; Osafune, T.; Motoyama, N.; Eisaki, H.; Uchida, S. Electronic states and magnetic properties of edge-sharing Cu-O chains. *Phys. Rev. B* **1998**, *57*, 5326. [CrossRef]
32. Atzkern, S.; Knupfer, M.; Golden, M.S.; Fink, J.; Waidacher, C.; Richter, J.; Becker, K.W.; Motoyama, N.; Eisaki, H.; Uchida, S. Dynamics of a hole in a CuO_4 plaquette: Electron energy-loss spectroscopy of Li_2CuO_2. *Phys. Rev. B* **2000**, *62*, 784. [CrossRef]
33. Kim, Y.-J.; Hill, J.P.; Chou, F.C.; Casa, D.; Gog, T.; Venkataraman, C.T. Charge and orbital excitations in Li_2CuO_2. *Phys. Rev. B* **2004**, *69*, 155105. [CrossRef]
34. Ebisu, S.; Komatsu, T.; Wada, N.; Hashiguchi, T.; Kichambare, P.; Nagata, S. Extremely large short-range order in an antiferromagnet Li_2CuO_2. *J. Phys. Chem. Solids* **1998**, *59*, 1407–1416. [CrossRef]
35. Ramos-Sanchez, G.; Romero-Ibarra, I.C.; Vazquez-Arenas, J.; Tapia, C.; Aguilar-Eseiza, N.; Gonzalez, I. Controlling Li_2CuO_2 single phase transition to preserve cathode capacity and cyclability in Li-ion batteries. *Solid State Ionics* **2017**, *303*, 89. [CrossRef]
36. Kawamata, S.; Okuda, K.; Kindo, K. ESR study on Li_2CuO_2 single crystal. *J. Magn. Magn. Mater.* **2004**, *272–276 Pt 2*, 939–940. [CrossRef]
37. Toby, B.H. EXPGUI, a graphical user interface for GSAS. *J. Appl. Cryst.* **2001**, *34*, 210–213. [CrossRef]
38. Cologne Laue Indexation Program. Available online: https://clip4.sourceforge.net/ (accessed on 17 February 2024).